Renewable Energy 207 (2023) 588–600

Contents lists available at ScienceDirect

Renewable Energy

journal homepage: www.elsevier.com/locate/renene

Influence of Lewis and Brønsted acid catalysts in the transformation of hexoses into 5-ethoxymethylfurfural

Benjamín Torres-Olea, Inmaculada Fúnez-Núñez, Cristina García-Sancho *, Juan Antonio Cecilia, Ramón Moreno-Tost, Pedro Maireles-Torres

Departamento de Química Inorgánica, Cristalografía y Mineralogía (Unidad Asociada al ICP-CSIC), Facultad de Ciencias, Universidad de Málaga, Campus de Teatinos, 29071, Málaga, Spain

ARTICLE INFO

Keywords:
Biofuel
Biomass conversion
5-(ethoxymethyl)furfural
Etherification
Ion-exchange resins
Alumina

ABSTRACT

Several sulfonated polymers, which are typical Brønsted acid catalysts, have been employed in the production of two biofuels: 5-ethoxymethylfurfural (EMF) and ethyl levulinate (EL) as main byproduct, and the catalytic results have been attributed to their different chemical and morphological properties. The Purolite CT275DR attained the best results from 5-hydroxymethylfurfural (HMF) with a 63% EMF yield after 16 h at 100 °C thanks to their more abundant superficial acid sites. Moreover, Purolite CT275DR was able to efficiently dehydrate and etherify fructose, with a total EMF plus EL yield of 65% after 24 h at 100 °C. When glucose or galactose were used as feedstock, alumina was utilized to provide Lewis acid sites, necessary for the transformation of aldoses in solution enabling a combined biofuel yield (EMF plus EL) of 40% from glucose after 24 h at 140 °C. With the study of the role of each catalyst, both Brønsted and Lewis acid catalysts (resin and alumina, respectively) were required to obtain considerable EMF yields from aldoses. The reutilization of the catalysts employed for 5 catalytic runs demonstrated that Purolite CT275DR suffers no appreciable loss of activity, but alumina showed progressive losses in activity in each cycle due to carbonaceous deposits and catalyst loss.

1. Introduction

The ever-threatening depletion of fossil resources together with environmental concerns are pushing for more sustainable and renewable resources, like biomass. This is expected to find a niche position providing materials for the production of polymers, intermediate chemicals and biofuels, and as energy source, alleviating our dependence on fossil resources on the short term and substituting them totally or partially in the long term [1]. Lignocellulosic biomass has been thoroughly studied as one of the best candidates given its abundance and extensive possibilities [2,3]. Lignocellulose is composed of 35–50% cellulose (β-D-glucose biopolymer), 20–35% hemicellulose (biopolymer of various pentoses and hexoses) and 10–25% lignin (a polyphenolic biopolymer). Therefore, lignocellulosic biomass is composed primarily out of saccharides in the form of biopolymers [4]. Additionally, algal biomass has attracted great interest due to its faster growth than terrestrial plants and does not require fertile land to grow. Furthermore, lignin is absent in algal biomass, which facilitates depolymerization of algal raw materials [5,6]. Instead of lignin and hemicellulose, other biopolymers make up for the composition of algae like laminarin, starch, agar, and others, which are abundant in glucose, galactose and dehydrogalactose [5]. Therefore, it is not questionable that saccharide mass valorisation is of utmost importance due to its abundance in the biosphere as a renewable resource.

In consequence, dehydration of hexoses has been extensively studied, yielding 5-hydroxymethylfurfural (HMF), a promising platform molecule from which a wide variety of products can be derived, among them: levulinic acid, formic acid, γ-valerolactone or 2,5-furandicarboxylic acid, biofuels, etc [7–10]. In the last years, one of the biofuels that has attracted the attention of researchers is 5-ethoxymethyl furfural (EMF), which can be synthesized from the simple etherification of HMF with ethanol in acid conditions. EMF shows a high energy density (30.3 MJ L^{-1}), high miscibility with fuels currently employed and improves the combustion in engines reducing carbonaceous particulate emission [11]. Its production results advantageous over other biofuels that can be also derived from HMF, given that there is no need to carry out a reduction step of this chemical under high hydrogen pressures, also avoiding the loss of energy density.

* Corresponding author.
E-mail address: cristinags@uma.es (C. García-Sancho).

https://doi.org/10.1016/j.renene.2023.03.036
Received 29 June 2022; Received in revised form 22 December 2022; Accepted 7 March 2023
Available online 12 March 2023

In general, it has been widely proposed that firstly hexoses have to be isomerised and dehydrated into HMF and then etherified into EMF [12, 13]. On the one hand, HMF and EMF have been produced with relevant yields from biomass through the utilization of high amounts of HCl, with 5-chloromethylfurfural as intermediate. Mascal et al. synthesized 5-chloromethylfurfural with a yield of 81% from glucose and even 80% from corn stover, which they could convert to EMF with a 95% yield [14, 15]. However, the handling of highly concentrated HCl solutions is associated with equipment corrosion and health and environmental concerns that make implementation difficult. On the other hand, heterogeneous catalysts are easily recoverable, active, and do not cause severe corrosion problems. Yang et al. utilized a niobium-molybdate layered catalyst that could etherify selectively (>99% yield) HMF with alcohols such as methanol and ethanol [16]. Collins et al. prepared sulfonated aluminium-zirconium mixed oxides supported over KIT-6, which provided both Lewis and Brønsted acids sites. They demonstrated higher zirconium loading to be favourable to the final EMF yield in the direct etherification of HMF, attaining a maximum EMF yield of 67% [17]. Changwei et al. synthesized organic sulfonated polymers that were subsequently used in the one-pot transformation of fructose to EMF, achieving a 69% yield at 140 °C after 18 h in ethanol:THF (3:1) solution, [18]. Liu et al. employed sulphonic acid supported over mesoporous silica [19]. Although the catalyst could dehydrate fructose and produce EMF with high yield (84% and 63% from HMF and fructose, respectively), it was not capable of converting glucose into EMF. In contrast, ethyl glucoside (EG) was produced in great quantity (92% yield).

Thus, it has been reported that fructose can be readily dehydrated into HMF and etherified using strong Brønsted acids but these sites regularly lead to the etherification of the anomer carbon in the case of the aldose glucose when it is employed as feedstock [19–23]. Therefore, although relevant EMF yields could be obtained from fructose, its production from aldoses such as glucose and galactose, which are present in different types of biomass like lignocellulosic or algae biomass, is more interesting but more difficult. To overcome that drawback it is necessary the presence of Lewis acid sites in the reaction medium, whose purpose is to isomerize aldoses to their correspondent ketoses, via hydride transfer [24]. Li et al. combined protonic and dealuminated zeolites with Amberlyst-15 to improve the catalytic performance, achieving up to 46% EMF yield in a one-pot two-step process, in which the reaction was stopped by cooling to add a second catalyst, before initiating the reaction again [25]. In the same way, Lew et al. employed jointly a Sn-Beta zeolite as Lewis acid catalyst for the isomerization of glucose into fructose, and a Brønsted acid resin (Amberlyst-131) to promote the dehydration of the ketose and the etherification reaction [13]. They introduced both catalysts in sequential order in such a way that they filtered Sn-Beta zeolite after 5 h and added Amberlyst-131, obtaining a final EMF yield of 31% after 24 h. It should be noted that each catalyst was incorporated in an independent step, not being a real *one-step* process. Xin et al. carried out the reaction using $AlCl_3$ as Lewis acid catalyst and combining it with PTSA-POM to provide Brønsted acid sites. This resulted in the production of 31% EMF and 12% HMF yield from glucose at 150 °C after 30 min in an ethanol–water (9 : 1) solvent system [26].

Therefore, a suitable combination between Lewis and Brønsted acid catalysts is crucial for EMF production from aldoses. In the present work, cation-exchange resins and alumina were employed as pure Brønsted and Lewis acid catalysts, respectively, to produce biofuels from biomass derivatives and evaluate the role of each type of acid sites. Firstly, the catalytic performance of several Brønsted acid resins was evaluated. In this sense, different commercial sulfonated polymers were tested in the etherification of HMF and production of biofuels from hexoses derived from biomass. Sulfonated polymers are interesting options for the valorisation of biomass, given their strong Brønsted functional groups allows these resins to act as active heterogeneous catalysts. Thus, Purolite CT275DR, Purolite CT269DR, Amberlyst-15DRY (macroreticular type resins) and Purolite PD206 (gel type resin) were evaluated in order to deepen about the influence of their properties on the catalytic performance and know which resin is more suitable for EMF production. Furthermore, the resin that yielded the best results was chosen for further research and optimization, as well as their activity in the conversion of fructose, glucose and galactose, by itself and together with the addition of acid alumina to provide Lewis acid sites to the process in order to maximize the EMF production from aldoses like glucose and galactose. The influence of both catalysts on the catalytic performances was studied in one-pot, incorporating both materials at the beginning of process, unlike other studies previously reported in the literature.

2. Experimental

2.1. Materials

The following solids were employed as acid catalysts as received: ion-exchange resins, such as Purolite CT275DR, Purolite CT269DR and Purolite PD206 obtained from Purolite. Amberlyst-15DRY (Fluka) and an acidic γ-Al_2O_3 (Alfa Aesar, Acidic Alumina Brockmann Grade I, 58 Å). HMF (99,9%), D-Glucose (99%), D-galactose (99%) and D-fructose (99%) were purchased from Sigma-Aldrich. Ethanol (96%) was obtained from VWR Chemicals.

2.2. Reaction procedure

All reactions for EMF production were carried out in batch reactors (glass pressure tube with thread bushing Ace, 15 mL). General reaction conditions were 5 mL of ethanol 96% as solvent, 0.1 g of HMF or 0.15 g of hexose, and 0.05 g of catalyst in such a way that the substrate:catalyst weight ratio were 2 and 3, respectively. Before heating, reactors were purged with N_2 to avoid unwanted processes that could lead to HMF polymerization. Batch reactors were introduced in a temperature regulated aluminium block with magnetic stirring.

In the case of reuse tests, the reaction liquid was decanted leaving the solids, Purolite CT275DR and/or γ-Al_2O_3 catalysts, in the reactor, followed by drying at 80 °C for 1 h, without washing and regeneration steps. Then, the catalysts were reused again without any treatment, after adding a new reaction mixture formed by 0.15 g of glucose and 5 mL of ethanol 96%.

In all cases, once the reaction was finished, the reactor was submerged in water at room temperature to stop the reaction. To guarantee the dissolution of all components in the reactor tube allowing their proper quantification by high performance liquid chromatography (HPLC), 2.15 mL of deionized water were added before homogenising and taking a sample. Liquid samples were analysed by means of JASCO HPLC. The different compounds were detected and quantified using both a multiwavelength detector (MD-2015) and a refractive index detector (RI-2031-PLUS). Previously, the different components in the matrix were separated through a Phenomenex REZEX Ca^{2+}-Monosaccharide (300 mm × 7.8 mm) heated at 70 °C by a column oven (CO-2065). Flow conditions employed were 0.4 mL min^{-1} of deionized and microfiltered water, provided by a quaternary gradient pump (PU-2089). Conversion, selectivity and yield were defined as followed (Equations (1)–(3)):

$$\text{Conversion}_X = \left(\left(\text{mol}_{\text{initialX}} - \text{mol}_{\text{finalX}}\right)\right) / \text{mol}_{\text{initialX}}\right) \cdot 100 \quad (1)$$

$$\text{Selectivity}_Y = \left(\text{mol}_{\text{finalY}} / \left(\text{mol}_{\text{initialX}} - \text{mol}_{\text{finalX}}\right)\right) \cdot 100 \quad (2)$$

$$\text{Yield}_Y = \left(\text{Selectivity}_Y \cdot \text{Conversion}_X\right) / 100 \quad (3)$$

The carbon balance was determined using the following equation:

$$\text{Carbon Balance} = \frac{\sum \text{mol}_i \cdot \frac{n_i}{6}}{\text{mol}_{\text{initial}}}$$

Where i represents each of the detected compounds and n_i was the

number of carbon atoms in the detected compounds.

2.3. Catalyst characterization

Elemental analysis of ion-exchange resins was carried out in a LECO CHNS932 analyzer (LECO Corporation, St. Joseph, MI, USA). The catalysts were burned at 1100 °C in oxygen.

The swelling ratio was calculated by adding 10 mL of the polymer studied into a 50 mL graduated tube. Then, the tube was filled with 40 mL of ethanol 96%. After 24 h, the new volume occupied by the polymer is measured. The swelling ratio is therefore calculated by the Swelled: Non-swelled volume ratios.

Textural properties of catalysts were studied employing N_2 adsorption-desorption isotherms at −196 °C, after evacuation at 100 °C and 10^{-4} mbar, utilizing an automatic ASAP 2020 from Micrometrics. Brunauer-Emmett-Teller (BET) [27] equation was employed to determine specific surface area considering a N_2-molecule cross section of 16.2 Å^2. The pore size distribution was calculated by the density functional theory model (DFT) by alumina catalyst and the pore diameter was calculated by BHJ method for resins [28].

X-ray photoelectron spectra were acquired with non-monochromatic Mg Kα radiation (300 W, 15 kV, 1253.6 eV) in a Physical Electronics PHI 5700 with a multichannel detector. Adventitious carbon at 284.8 eV was used to calibrate the measurements, taken in pass-energy mode at 29.35 eV and a diameter area of 720 μm. Spectra were acquired and treated using a PHI ACCESS ESCA-V6.0 F software package. A Shirley type background was subtracted from the signals. Peaks were fitted using a Gaussian-Lorentzian curve.

Thermogravimetric analysis was performed by a TGA/DSX 1 model (Mettler-Toledo) under 50 mL min^{-1} air flow. Heating ramp was set to 10 °C·min^{-1} and the sample were analysed from 30 to 900 °C.

Fourier Transformed Infrared Spectroscopy Analysis (FTIR) was carried out in a Shimadzu Fourier Transform Infrared Instrument (FTIR8300). The catalyst was compacted into self-supported wafers, with a mass surface ratio of 15 mg cm^{-2}, that was evacuated at 300 °C and 10^{-2} Pa overnight. The wafer was exposed to a pyridine atmosphere (pyridine vapor pressure of 200 mbar) for 10 min, before outgassing at room temperature, 100 °C and 200 °C.

Temperature-programmed desorption of ammonia was used to quantify the total acidity of alumina. Prior to the analysis, 0.08 g of the solid was heated under a helium stream at 550 °C, to remove any superficial impurities. After that the sample was cooled under He flow and then ammonia was adsorbed on the catalyst at 100 °C. Then, temperature was increased from 100 °C to 550 °C, under 40 mL min^{-1} helium flow. Desorbed ammonia was quantified using a Shimadzu GC-14A Gas Chromatograph equipped with a thermal conductivity detector (TCD).

3. Results and discussion

3.1. Characterization and properties of heterogeneous catalysts

3.1.1. Sulfonated polymers

Cationic exchange resins studied in this work possess polystyrene structure crosslinked with divinylbenzene and functionalized with sulfonic groups that provide them with strong Brønsted acidity. In order to know the influence of resin type, macroreticular resins like Purolite CT275DR, Purolite CT269DR and Amberlyst-15DRY, and gel resin like Purolite PD206 were compared. Their elemental analysis reveals that all the polymers have a similar sulphur content, ranging from 12.8 wt% for the Purolite CT275DR to 13.8 wt% for the Amberlyst-15DRY (Table 1). These resins also showed similar values of ion-exchange capacity, as supplied by the provider, but a correlation between their dry weight capacity and sulphur content was not found.

Likewise, the sulphur content on the catalyst surface was determined by XPS (Table 1). Notably, Purolite CT275DR showed the highest superficial sulphur content (19.8 wt%), being much higher than that found by CHNS analysis which demonstrates high sulfonic group content on the catalytic surface of this resin. On the other hand, it should be noted that the lowest value was found for Purolite CT269DR, with only a 9.9 wt%. Purolite PD206 and Amberlyst-15DRY presented 14.9 wt% and 13.7 wt% respectively, a middle ground between the Purolite CT275DR and Purolite CT269DR. The chemical states of the different components of the polymers were also studied by XPS (Table S1, Fig. S1). It can be observed that three contributions were found in the C 1s region: the first signal at 284.8 eV corresponded to adventitious carbon (C–C, C–H), another signal at 286 eV was ascribed to both the carbon in divinylbenzene groups (C═C) with electron withdrawing groups, hydroxyl groups (C–OH) and sulphur bonded carbon (C–S), and the third signal, found at 287 eV, produced by carbonyl groups (C═O) in the polymer [29–32]. O 1s core level spectra presented two bands: the first, at 532 eV, is caused by the oxygen in sulfonic groups, while the other signal, at 533.6 eV, is caused by physisorbed water over the hydrophilic centres of the polymer [32]. The doublet in the sulphur region is caused by the sulfonate groups on the aromatic rings [29,30].

Table 1
Dry weight capacity and sulphur content of the sulfonated polymers.

	Dry weight capacity (meq H^+ g^{-1})[a]	Swelling ratio	Sulphur content by elemental analysis (wt%)	Sulphur content by XPS (wt%)
Purolite CT275DR	5.2	1.49 ± 0.02	12.8	19.8
Purolite CT269DR	5.2	1.38 ± 0.03	13.3	9.9
Purolite PD206	4.9	2.55 ± 0.06	12.9	14.9
Amberlyst-15DRY	4.7	1.68 ± 0.09	13.8	13.7

[a] Provided by the supplier.

On the other hand, the catalytic activity of a resin also depends on the accessibility of reagents into its matrix. Thus, the textural properties of these resins were evaluated by N_2 adsorption-desorption isotherms (Fig. S2). Thus, the macro-reticular polymers exhibited values of BET surface area between 26 and 44 m^2 g^{-1} (Table 2). The resins present mesoporosity that facilitates diffusion to and from active sites, with an average pore diameter ranging between 7.7 and 12.4 nm, as determined by BHJ method, being the lowest value found for Purolite CT275DR (Table 2).

However, N_2 adsorption–desorption isotherms only provide information about dry catalysts. Considering that the accessibility to the inner resin active sites varies in function of reaction medium since resins can swell due to solvent absorption, considerably expanding their volume, their study in the reaction media is a key factor [32]. Many morphological studies of resins have concluded that the most important factors to consider that affect activity and selectivity are the quantity of acid sites, along with of the expanded polymer volume in the solvent [33]. The swelling ratio for macro-reticular resins were determined, obtaining values of 1.68, 1.49 and 1.38 for Amberlyst-15DRY, Purolite CT275DR and Purolite CT269DR, respectively (Table 1). The swelling ratio found for the Amberlyst-15DRY was very similar to the ratio reported by Soto et al. [33]. In the case of the gel type resin, its morphology allows for a swelling of 2.55, almost triplicating their initial volume. This is favourable for exposing their active centres in the reaction media and improve diffusion.

Another key aspect is their thermal stability since it limits their applications at high reaction temperatures required for these reactions. It can be observed that Purolite CT275DR and Purolite CT269DR are the most stable, with a maximum operational temperature of 180 °C, while the gel type resin Purolite PD206 is only useable up to 120 °C (Table 2). Amberlyst-15DRY remains stable up to 120 °C in non-aqueous solution.

SEM micrographs revealed that all fresh resins, both macroreticular and gel type, are formed by spherical particles with a homogeneous

Table 2
Physical properties of the ion-exchange resins.

	Structure	Particle size (μm)[a]	BET Surface area ($m^2\ g^{-1}$)[b]	Pore Diameter Average (nm)[c]	Maximum operating temperature (°C)[a]
Purolite CT275DR	Macro-reticular	425–1200	26	7.7	180
Purolite CT269DR	Macro-reticular	425–1200	40	10.6	180
Purolite PD206	Gel	300–1200	0.5	10.4	120
Amberlyst-15DRY	Macro-reticular	300–425	44	12.4	120[d]

[a] Provided by the supplier.
[b] Calculated by BET.
[c] Calculated by BJH method using the adsorption branch.
[d] In non-aqueous media.

distribution (Fig. 1).

3.1.2. Alumina

Textural properties of alumina were determined from its N_2 adsorption-desorption isotherm at −196 °C. The analysis provided a specific surface area of 158 $m^2\ g^{-1}$. The adsorption-desorption isotherm can be classified as Type IVa (Fig. S3a), according to IUPAC, which is typical of mesoporous materials in which the adsorbate condenses in mesopores. The hysteresis resembles H2(b), where pore blockage or percolation takes place in mesopores of varied neck widths. Pore distribution calculated by DFT (Fig. S3b) shows pore widths ranging from 2 to 10 nm, with most of the pore area concentrated around 5 and 6 nm width pores. Only pores wider than >0.9 nm are able to accept a sugar molecule in their cavity and facilitate its interaction with acid sites. However, it has been reported that introduction of molecules in pores results in reduced selectivity by promotion of high molecular weight polymeric materials [34,35]. The study of temperature-programmed desorption of NH_3 (NH_3-TPD) (Fig. S4) revealed a high concentration of acid sites (478 μmol $NH_3 \cdot g^{-1}$) for alumina. The NH_3-TPD curve also showed the existence of acid sites of different strength. A superior intensity of the desorption band at 160 °C reveals that weak acid sites are the most abundant on the surface, but desorption of ammonia molecules extends up to 550 °C, the maximum temperature at which the analysis has been carried out. FTIR spectra, after pyridine adsorption, showed vibration bands at 1614, 1593, 1578, 1493 and 1449 cm^{-1} (Fig. S5). After evacuation at 100 °C, the band at 1593 cm^{-1} almost disappears. This is caused by the elimination of the contribution of the weakly physisorbed pyridine, which, as previously reported, gives rise to signals at 1590, 1580, and a doublet at 1445-1439 cm^{-1} [36]. Still, after evacuation at 200 °C, the four characteristic bands associated to Lewis acid sites are identified in the spectra at 1614, 1593, 1493 and 1449 cm^{-1}, associated to the vibration modes 8a, 8b, 19a and 19b of the C–C–N of the pyridine. Therefore, we can unambiguously claim the Lewis acidity of this alumina catalyst [36,37].

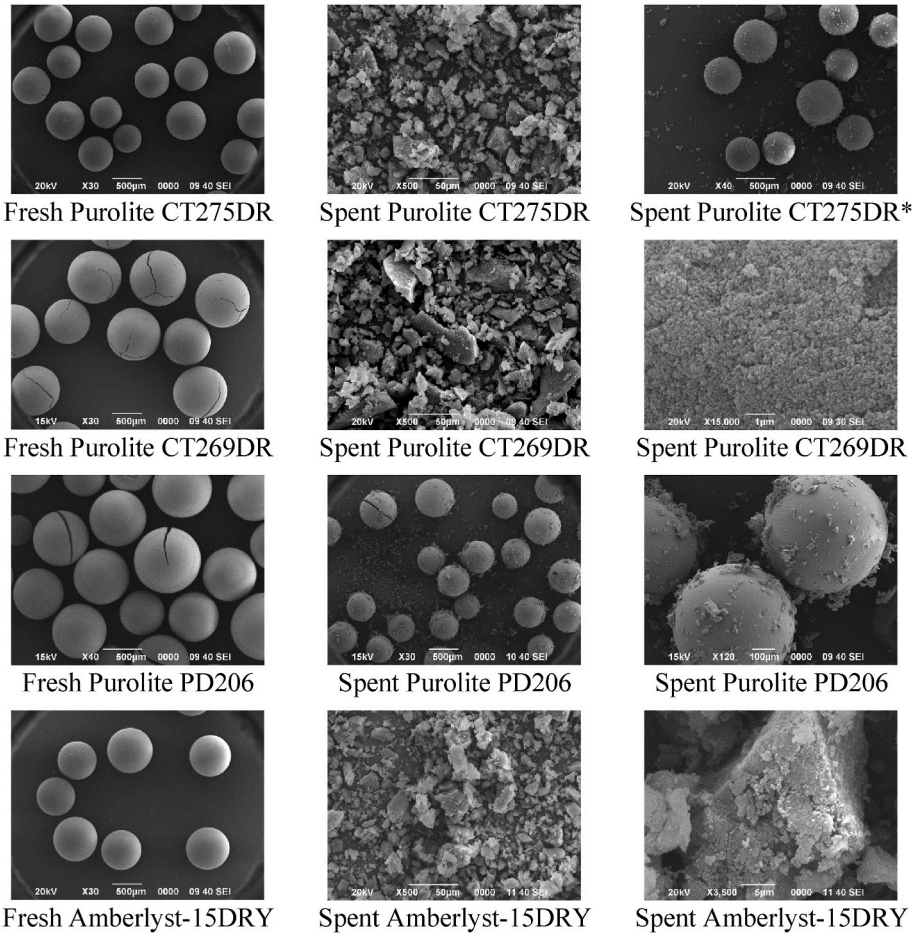

Fig. 1. SEM images of resins before and after the catalytic test at 1400 rpm, 100 °C and 3 h (*after use at 250 rpm at 100 °C and 3 h).

3.2. Screening of commercial resins in the HMF etherification

Firstly, the ion-exchange resins were employed as heterogeneous catalysts for HMF etherification in order to evaluate the influence of morphology and physicochemical properties of these sulfonated polymers on the EMF production. Thus, a kinetic study was carried out at 100 °C to evaluate their catalytic activity (Fig. 2).

Regarding HMF conversion values (Fig. 2a), Purolite CT275DR and Purolite PD206 seemed to be slightly more active than the others, producing higher HMF conversion and yield values than Purolite CT269DR and Amberlyst-15DRY. It should be noted that, under these experimental conditions, the lowest activity values were found for Purolite CT269DR. Despite possessing the same concentration of acid sites than Purolite CT275DR, according to data provided by the supplier (Table 1), XPS analysis points out that Purolite CT275DR exhibited a higher content of superficial sulphur than Purolite CR269DR (19.8 wt% versus 9.9 wt%). This large difference in number of available sulfonic groups on the catalyst surface could thus explain its lower activity with respect to Purolite CT275DR. In addition, the swelling ratio for Purolite CT275DR was slightly higher than value found for Purolite CT269DR, which could have influence on the number of available sites in ethanol medium for these resins. Amberlyst-15DRY was also found to have a smaller number of superficial active sites than Purolite CT275DR by XPS. Thus, the highest surface S content determined by XPS for Purolite CT275DR, combined with its swelling, allowed it to obtain higher values of conversion and yields than the rest of macroreticular polymers. On the other hand, Purolite PD206 displayed a 14.9 wt% of superficial sulphur content. This resin has exhibited the highest swelling ratio respect to any other studied resin by an ample margin. Therefore, Purolite PD206 exposes a larger number of active sites than possible for the macroreticular sulfonated polymers. The high swelling compensates for the lesser superficial sulfonic acids and allowed the Purolite PD206 to produce EMF yields comparable with the Purolite CT275DR, and even to provide higher EL yields.

On the other hand, HMF conversion followed a first order reaction (Fig. 2d) with very high conversion values after 24 h of reaction for all studied resins. In all cases, the main product detected was EMF, whose yield increased along reaction time, being maximum (63%) in the presence of Purolite CT275DR after 16 h of reaction (Fig. 2b). However, it should be mentioned that all resins achieved an EMF yield close to 60% after 24 h. When most of the HMF had already been consumed, and EMF production halted, from 16 to 24 h depending on each catalyst, only a small decrease in EMF yield was observed. This slight decrease confirms the great stability of the etherified furan, which is barely affected by secondary reactions. It should be also noted that HMF conversion and yield attained with Purolite CT275DR and PD206 surpass those obtained with Amberlyst-15DRY.

Likewise, HMF and EMF rehydration are known to produce levulinic and formic acids, or their respective esters in alcohol media [38]. Over time, EL yield increased in agreement with this statement (Fig. 2c). Indeed, ethyl levulinate was detected as main by-product. It can be observed that while Purolite CT275DR, CT269DR and Amberlyst-15DRY presented similar values of EL yield, Purolite PD206 showed an especially high EL selectivity, with an EL yield of 26% after 24 h. Thus, the Purolite PD206 favoured the HMF rehydration, as inferred from its high EL yield. As mentioned before, the higher swelling ratio found for

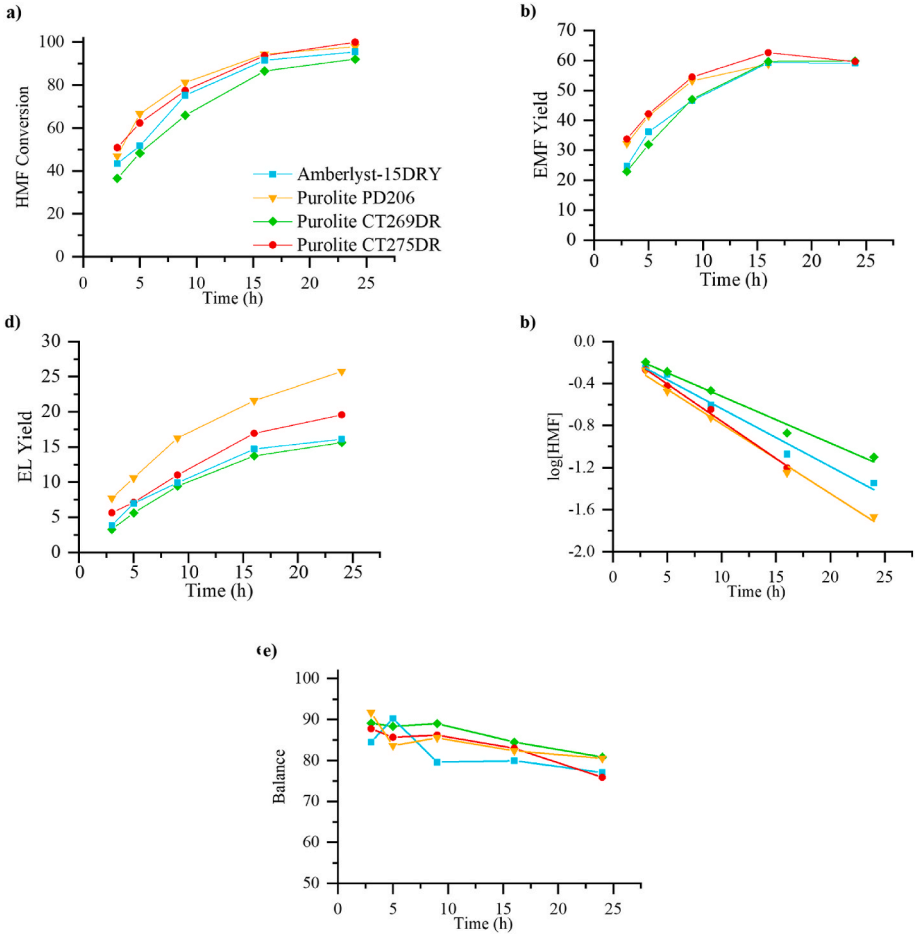

Fig. 2. a) Conversion of HMF, b) EMF yield, c) EL yield, d) logarithmic representation of HMF concentration and e) carbon balance, as a function of reaction time (Experimental conditions: 100 °C, 0.1 g HMF, 0.05 g catalyst and 5 mL ethanol).

Purolite PD206 indicates that a high quantity of active sites can be exposed in the reaction medium that, in turn, catalyse the rehydration of HMF and EMF into EL with more ease than the other materials. Therefore, it can be deduced that the effect of catalyst morphology plays an important role in product selectivity and HMF rehydration. Finally, it can be observed that carbon balance was similar in all cases (Fig. 2e). Thus, different resins exhibited a carbon balance about 90% at the first hours of the reaction, which was only reduced to about 80% after 24 h of reaction.

On the other hand, HMF conversion and EMF yield values attained in these experiments were higher than those values reported by Che et al. [39], who achieved a EMF yield of 16% after 4 h at 90 °C by using Amberlys-15 as catalyst. They also detected 5,5′ (oxy-bis(methylene)) bis-2-furfural (HMF dimer) and EL with selectivities of 12.4 and 5.2%, respectively. In our case, HMF or EMF dimers or acetals were not produced in detectable quantities, as reported by several publications [39–42]. Bell et al. reported a yield of 31% for 5-ethoxymethyl diethyl acetal, after 24 h of reaction at 75 °C in the presence of Amberlyst-15 [41]. This difference could be explained by the higher temperature used in the present work, that would affect unfavourably the formation of the acetal [43].

After these reactions, it was observed that the rounded particles lost their spherical structure and particle size was diminished. Considering that some of fresh resins presented visible cracks in the microspheres, they were recovered after reaction for 3 h at 100 °C under 1400 rpm and studied by SEM (Fig. 1). Amberlyst-15DRY and Purolite CT269DR, together with Purolite CT275DR were not mechanically stable under 1400 rpm. The gel type resin, Purolite PD206, was the only resin that endured high rates despite having the less divinylbenzene content. The macro-reticular resins are composed of many micro-sized gel-type spheres. The mechanical forces of the stirring cause the micro-spheres to break free and the macro-reticular structure disintegrates. This problem is absent in compact gel type resins [44]. Therefore, the larger particle sizes of macro-reticular resins could be responsible of their lower mechanical stability, as was mentioned by Ginés-Molina et al. [45]. Thus, functionalized crosslinked polymers are vulnerable to mechanical stress, in such a way that stirring rate could cause the breakdown of catalyst particles, which may be source of reproducibility issues. For this reason, the influence of the stirring rate was studied with Purolite CT275DR. However, no significant differences were found in the activity or product distribution (Fig. S6). 250 rpm was deemed the most appropriate stirring rate to avoid particle breakdown and conserve their spherical structure, which facilitates manipulation, separation from the solvent and reutilization (Fig. 1*). Moreover, elemental analysis could not detect any loss in sulphur content in the sulfonated polymer or in the reaction media after submitting fresh Purolite CT275DR for reaction for 5 h at 100 °C and 1400 rpm. This would indicate that leaching does not occur under these experimental conditions, or at least it does not occur to an appreciable extent.

Therefore, Purolite PD206, which presented the best total EMF plus EL yield among the tested resins (73% biofuel yield at 24 h), exhibited the highest stability under high stirring rate values. However, Purolite PD206 gel type resin is considerably sensitive to temperature, being recommended by the provider not to exceed 120 °C. Purolite CT275DR originated a similar EMF yield, although total EMF plus EL yield (69% at 24 h) was slightly lower than that obtained for Purolite PD206. Hexoses are more difficult to convert than HMF, and more severe experimental conditions will be required to achieve a suitable catalytic performance from hexoses, therefore, Purolite CT275DR was selected to continue this study. Thus, several experimental parameters were modified to assess their effect on the catalytic activity, such as reaction temperature, the catalyst loading, the EMF production from hexoses as well as the reuse of catalyst.

3.3. HMF etherification and hexoses dehydration using Purolite CT275DR as catalyst

3.3.1. Influence of temperature on HMF etherification

Firstly, reaction temperature was varied between 80 and 120 °C and its effect was evaluated throughout the 24 h reaction for HMF etherification in the presence of Purolite CT275DR, keeping constant the rest of the parameters (Fig. 3). As expected, using higher temperatures increased conversion rate. Thus, full HMF conversion was attained after 24 h of reaction at 100 °C (Fig. 3a). However, the consumption of HMF only required 5 h of reaction to be complete at 120 °C. The maximum operating temperature of this resin is 180 °C (Table 2), being completely feasible to carry out the etherification reaction at 120 °C without risking thermal degradation of the resin. Moreover, the highest EMF yield was reached at 120 °C, achieving a value of 60% after only 3 h of reaction before declining in a short lapse of time down to 58% at 5 h and 39% at 24 h (Fig. 3b). At 100 °C, longer reaction times were required to attain similar EMF yield values, obtaining an EMF yield of 63% after 16 h of reaction. However, EMF yield decreased along reaction time, in a seemingly linear way at 120 °C. This enhancement of HMF conversion and decrease of EMF yield with the reaction temperature was also observed by Liu et al. in the presence of silica-SO_3H catalysts [19]. They affirmed that a higher reaction temperature provoked more side reactions, mainly the polymerization of HMF and the formation of ethyl levulinate. This same fact was found in the presence of Purolite CT275DR, in such a way that EL yield increased and reached up to 35% after 24 h at 120 °C, while its formation was less relevant at lower temperatures (Fig. 3c). In addition, carbon balance was negatively affected by temperature. This demonstrates that higher temperatures favour the rehydration and polymerization of furans.

However, there still was the question whether the protected EMF could be rehydrated into EL, or it was solely produced from HMF in solution. This was checked by putting in contact 800 μmol of EMF with 0.05 g of Purolite CT275DR for 24 h at 100 °C, in ethanol (5 mL) (Fig. S7). EL was produced with a 9.5% yield, with a 29% of conversion. This value is lower than the EL yield value obtained when using HMF as feedstock. Moreover, the carbon balance is also better in this case. Therefore, it can be deduced that, although EMF is also vulnerable to undergo secondary processes that lead to rehydration and polymerization, the etherified form of HMF is more stable to decomposition and rehydration than its un-etherified counterpart, as carbon balance is greater in the case of using EMF instead of HMF (80% against 71%, respectively).

3.3.2. Conversion of hexoses into EMF

Therefore, it has been demonstrated that Brønsted acid sites existing in Purolite C275DR were able to catalyse the HMF etherification, being EMF the main product detected with high yield values. However, it is important to achieve the direct transformation of hexoses to EMF instead of utilizing HMF as feedstock, given that these carbohydrates are widely available from biomass resources, such as lignocellulose or algae. Hence, Purolite CT275DR was tested by using fructose, glucose, and galactose as feedstocks to obtain EMF in a one-pot reaction (Fig. 4). The catalytic data revealed that fructose was readily dehydrated in the presence of strong Brønsted acid sites present on sulfonated resins, giving rise to a HMF yield of 40% after 3 h, which rapidly decreased due to the formation of EL and, mainly, EMF (Fig. 4a). Thus, an EMF yield of 52% was achieved from fructose after 24 h in the presence of Purolite C275DR, together with an 8% HMF yield and a 14% EL yield, with a 74% carbon balance. Under similar experimental conditions, when HMF was used as feedstock, the EMF Yield obtained was 60%. Considering that fructose dehydration could lead to an EMF yield of 52%, that would mean that fructose dehydration to HMF took place with a selectivity of at least 87%. Zhang et al. found very low EMF yield (5.1%) from fructose, after 4 h at 120 °C, using another cationic exchange resin, Amberlyst-15, as acid catalyst [46]. Morales et al. detected a higher EMF

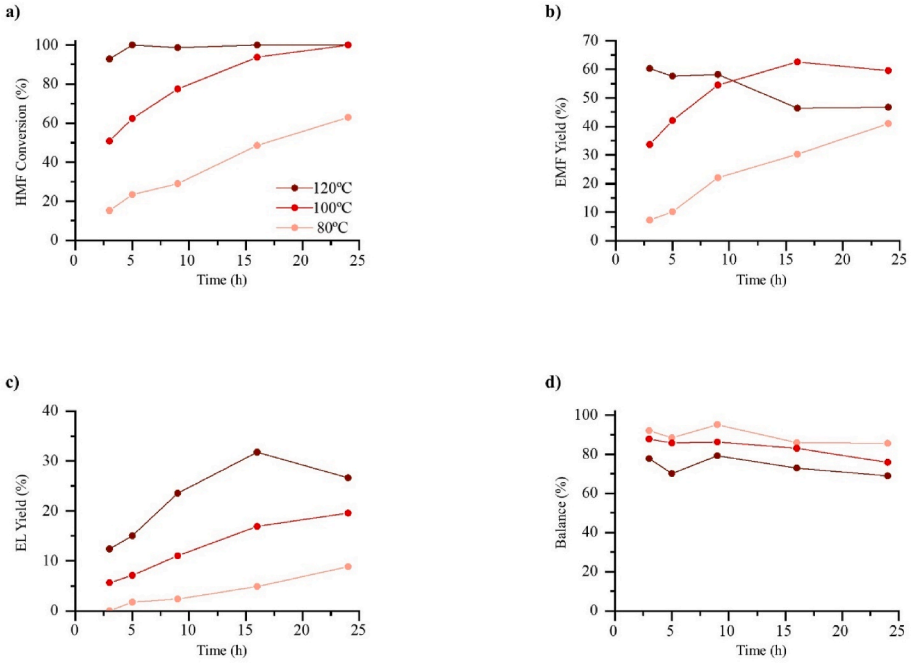

Fig. 3. Effect of reaction temperature along reaction time on: a) HMF conversion, b) EMF yield, c) EL yield and d) carbon balance (Experimental conditions: 0.1g HMF, 0.05 g Purolite CT275DR, 5 mL ethanol).

yield (22%) using this same resin and carrying out this reaction from fructose at 110 °C for 8 h [47], being lower than that value found in this work using Purolite C275DR. Likewise, Maneechakr et al. used a sulfonated carbon, obtaining an EMF yield of 32% at 120 °C after 6 h in ethanol, using fructose as feedstock [48]. Ge et al. prepared a carbon-based sulphonated catalyst, which was tested under microwave radiation for the dehydration of fructose to EMF. At 75 °C, the catalyst achieved a 61.2% EMF yield with 80.3% fructose conversion, under 110 W of microwave radiation [49]. Recently, Dowaki et al. synthetised a lignin-derived biochar catalysts functionalized with sulfonic groups. The transformation of fructose was carried out at 115 °C for 6 h in ethanol medium and was able to provide a 66% EMF yield, as well as moderate yields of HMF and EL (11% and 22%, respectively) [50]. Therefore, relevant EMF yields were obtained using Purolite C275DR as acid catalyst from fructose in comparison with others previously reported in the literature.

However, when other hexoses, such as glucose and galactose, were employed as feedstocks, only traces of HMF, EMF and EL were detected (Fig. 4b and c). Although the mechanism of glucose dehydration continues to be somewhat polemic and unclear, in general, it is accepted that glucose transformation occurs via the isomerization to fructose, before dehydrating to HMF [51,52]. To this purpose, the presence of Lewis acid or basic sites are needed to promote the enediol formation or hydride shift isomerization from the aldose to the ketose form [53]. From there forth, fructose dehydration takes place normally on Brønsted acid sites. The mechanisms behind galactose dehydration are much more unclear, though presumably the same could be also applicable to this aldose. It has been identified the presence of tagatose as intermediate to HMF, when galactose was employed as feedstock [54]. Therefore, due to the lack of Lewis acid sites, aldoses were converted into their etherified forms, ethylglucopyranosides (EGp) and ethylgalactopyranosides (EGalp), in both, their α and β forms, instead of dehydrated to HMF.

In our case, aldose etherification took place very fast compared to dehydration of fructose or etherification of HMF. Thus, galactose etherified completely in the first 3 h of reaction with a yield over 97%. On the other hand, glucose etherification was slightly slower, with 78% EGp yield. No by- products were detected in either case. These results agree with those found by Pinheiro et al., who demonstrated that silicotungstates exchanged with tin were active in the ethanolysis of fructose, but they failed when aldoses, like glucose and galactose, were employed as feedstock, instead, being converted to unspecified products [55]. Zhong et al. came to a similar conclusion, demonstrating that the absence of Lewis acid sites in silica-carbon sulfonated mesostructured composites led to the formation of ethylglucoside (EG) from glucose, instead of evolving to fructose and, subsequently, to HMF and EMF [56]. Likewise, Zang et al. prepared sulfonic polymer microspheres for the production of EMF from fructose and glucose [46]. Zang et al. could attain a 67% EMF yield from fructose, after 2 h at 150 °C. However, EMF could not be produced from glucose due to the lack of Lewis acid sites.

It should be also noted that the α and β forms were found in different proportions in the case of glucose and galactose. On the one hand, the α- and β-ethylgalactopyranosides were formed in an almost 1:1 ratio. On the other hand, in the case of glucose etherification, it is interesting to note that β ethylglucopyranoside was formed preferentially in the first hours of the reaction. As the process continued, the α anomer grew in proportion respect to the β anomer, until a α:β relation close to 2:1 was achieved (Fig. S8). Therefore, the formation of the β-ethylglucopyranoside isomer is favoured from a kinetic point of view, but the α isomer is the thermodynamically favoured. The explanation to the superior α isomer stability is caused by the anomeric effect, since α substituents have hyperconjugation effects that stabilize the axial position [57]. On the other hand, β isomers suffer from unstable interaction between the $–OCH_2CH_3$ electron pair and the pyranose ring's oxygen. However, the only difference between galactose and glucose is the configuration of the C_4; therefore, the orientation of this hydroxyl group must play a key role in defining the final configuration of the anomeric carbon. This must be caused by anchimeric participation of the hydroxyl in position 4, assisting the attack by the upper face of the pyranose ring.

3.4. Conversion of hexoses using Purolite CT275DR in the presence of alumina

Once demonstrated the inability of Brønsted acid sites for aldose conversion to HMF and, subsequently, EMF, it was proceeded with the addition of a catalyst that provided Lewis acid sites to promote

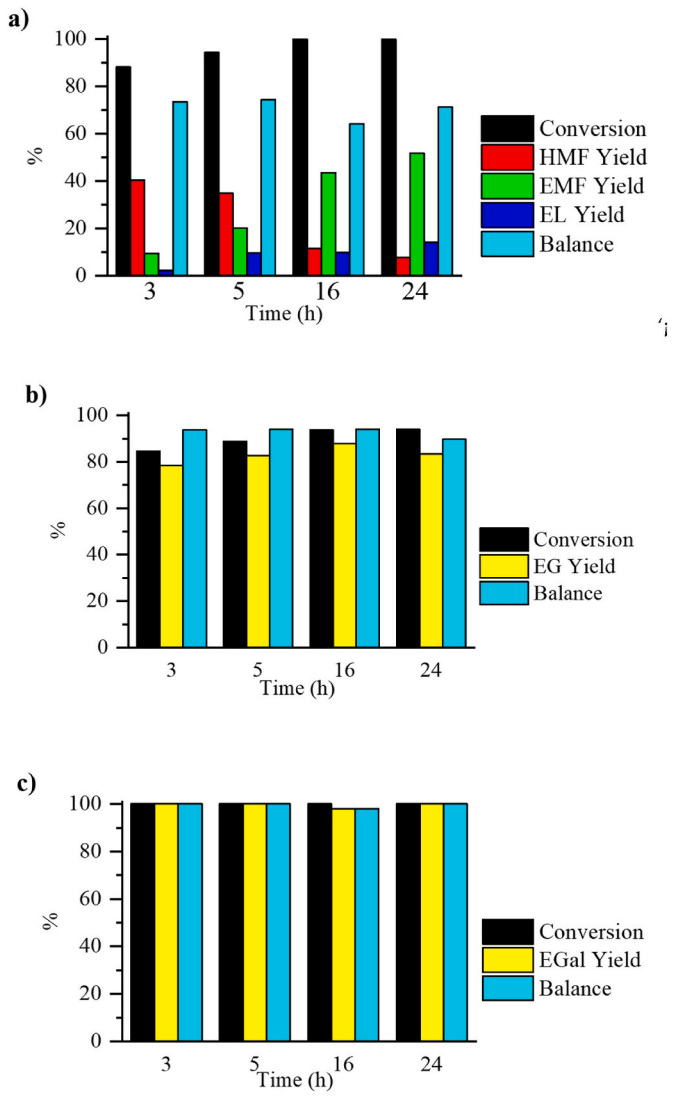

Fig. 4. Influence of reaction time on conversion and yield values in the presence of Purolite CT275DR by using: a) fructose, b) glucose and c) galactose, as feedstock (Experimental conditions: 0.15 g hexose, 0.05 g Purolite CT275DR and 100 °C).

isomerization of aldoses into ketoses and, therefore, allowing aldoses to be dehydrated in the reaction medium. Thus, an acidic γ-Al_2O_3 was chosen to study the interaction of hexoses with a typical Lewis acid solid in ethanol media. Firstly, the catalytic behaviour of this acid alumina by itself was performed between 100 and 140 °C in ethanol medium (Fig. S9). When using fructose as feedstock, glucose was found at all temperatures, therefore, alumina is isomerising fructose to the aldose. It can be observed that fructose was not dehydrated using alumina between 100 and 120 °C, since only at 140 °C, HMF could be detected with 11% yield (Fig. S9a). EMF could not be found, indicating that Lewis acid sites on γ-Al_2O_3 are unable to etherify HMF. When glucose was employed as feedstock in the presence of γ-Al_2O_3 (Fig. S9b), a mixture of α- and β-ethylglucofuranoside yield of 23%, corresponding to a selectivity of 81%, was found after 3 h at 100 °C. The further increase in temperature led to a decrease in the selectivity towards ethylglucofuranosides at 140 °C, in favour of the dehydration of the reactants to HMF (6% HMF yield), but no etherification to EMF took place. Thus, dehydration to form HMF can occur in the absence of strong Brønsted acid sites on the catalyst. However, without these strong Brønsted acid sites, HMF etherification could not take place, since neither EMF nor EL could be detected in the reaction media. Therefore, Lewis acid sites existing in this alumina were able to isomerize glucose into fructose, in ethanol medium. Also, Lewis acid sites were able to dehydrate hexoses to HMF, but they were incapable of etherifying to EMF.

Considering that the presence of alumina allowed us to produce HMF when utilizing glucose as feedstock, a mixture of alumina and ion-exchange resin was employed in order to promote the EMF formation from different hexoses, evaluating this catalytic process at different temperatures (Fig. 5).

Thus, the total substrate:catalyst weight ratio was 3:2. When fructose was employed as feedstock (Fig. 5a), a similar catalytic performance was found in the presence of both alumina and resin than that obtained in the presence of only the resin at 100 °C (Fig. 4a). This fact demonstrates again that alumina did not promote the EMF production. Therefore, HMF etherification is mainly accomplished on Brønsted acid sites, unlike that proposed by Lanzafame et al., who affirmed that Lewis acid sites

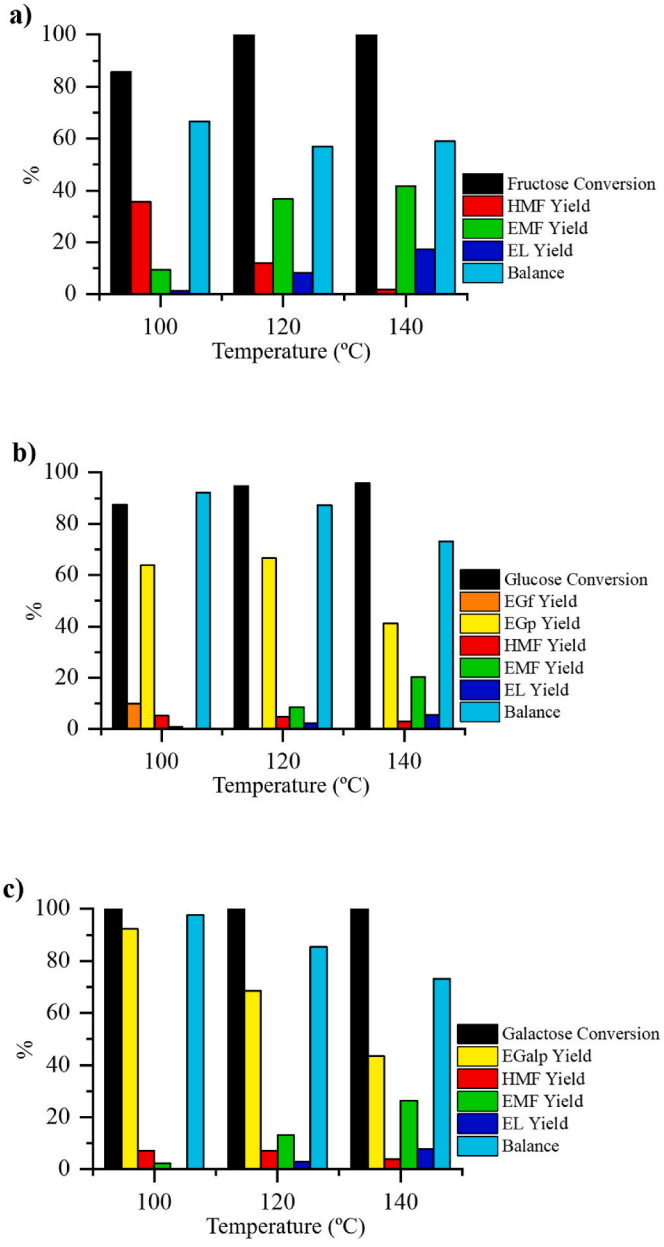

Fig. 5. Influence of reaction temperature on conversion and yield values in the presence of γ-Al_2O_3 and Purolite CT275DR by using: a) fructose, b) glucose and c) galactose, as feedstock (Experimental conditions: 0.15 g hexose, 0.05 g Alumina, 0.05 g Purolite CT275DR and 3 h).

enhanced the EMF production from HMF ($y_{EMF} = 68\%$) with Al-MCM-41 for 5 h at 140 °C [58].

On the other hand, when glucose was employed as reactant, ethylglucofuranosides were only detected at 100 °C, which represents 10% of the total carbon balance, but they were not present at 120 or 140 °C. This would suggest that ethylglucofuranosides produced from glucose are unstable and are consumed rapidly at higher temperatures. It can be observed that glucose conversion enhanced with reaction temperature, whereas galactose conversion was almost complete for all temperatures (Fig. 5b and c). The addition of alumina affected negatively to ethylglucopyranoside yield: 78% with only Purolite CT275DR versus 63% when alumina was added, at 100 °C. Ethylglucoside production was promoted by increasing the temperature from 100 °C (63%) to 120 °C (67%), but decreased to 41% with a higher reaction temperature (140 °C) due to increased reaction rates, as those leading to dehydration, as inferred from increased EMF yield. At 140 °C, 20% EMF yield was produced from glucose. Concurrently, HMF, EMF and EL were detected in the presence of both catalysts, γ-Al_2O_3 and Purolite CT275DR, by dehydration of glucose and subsequent HMF etherification. In the case of EL, it started to be detected at 120 °C, also increasing its selectivity with reaction temperature. Galactose behaved in a similar way, and, after 3 h at 140 °C, EMF yield reached 26% (Fig. 5c). However, EL yield did not exceed 8% in any case, under the reaction conditions studied.

As the highest EMF yield obtained from hexoses, in the presence of γ-Al_2O_3 and Purolite CT275DR, was attained at 140 °C, the influence of reaction time was evaluated at this temperature by using both catalysts (Fig. 6).

In the first hour, a glucose conversion of 80% was achieved, although only a 10% EMF yield was detected. Both glucose conversion and EMF yield enhanced along reaction time, in such a way that, with 97% glucose conversion, EMF yield reached 26% after 24 h. This result is similar to that found by Zhang et al., who synthesized a porous coordination polymer by self-assembly, with Brønsted and Lewis acid sites, provided by sulfonic groups and Cr^{3+} cations, respectively [59]. This catalyst produced a 23% EMF yield under the optimised conditions from glucose, using an ethanol-water system at 140 °C for 22 h. If Fig. 6 is compared with Fig. 4b, it can be seen that the presence of alumina favoured the formation of EMF instead of EG, due to the presence of Lewis acid sites, which promoted the glucose isomerization. It should be noted that HMF yield remained low, being consumed rapidly after its formation to produce EMF. However, EMF yield was enhanced from 1 to 3 h, but, then, it remained almost unchanged. With a 45% of glucose and ethyl glucopyranosides (EGp) combined yield after 3 h reaction, a EMF yield of 20% was achieved, but the conversion of the remaining 45% hardly produced 6% of extra net EMF in the following hours. The ratio between α:β EGp was also constant, with a value of 2 under these experimental conditions. Ethyl glucofuranosides (EGf) were detected with 2% yields at 1 h (not shown), but was no longer present in the analysis of longer reaction times. Regarding EL yield, it also started to increase as reaction time progressed. Thus, although only a value of 1% was detected for 80% glucose conversion after 1 h, over time rehydration took place, which caused EL yield to steadily rise up to 18% after 24 h. Therefore, EMF could be partially converted to EL as was detected in *Section 3.3.1*. Hence, after 24 h, the combination between Purolite CT275DR and Al_2O_3 led to a 42% biofuel (EMF plus EL) yield from glucose, as well as 5.5% yield HMF. On the other hand, more than 20% of the carbon balance remained unaccounted for in the first hour, which steadily declined over time, despite the quantification of all major peaks present in the chromatogram. This same fact was observed in Fig. S9, when glucose dehydration was carried out using only alumina as acid catalyst. Therefore, it would be possible that glucose and/or some reaction products remained adsorbed on Lewis acid sites existing on alumina.

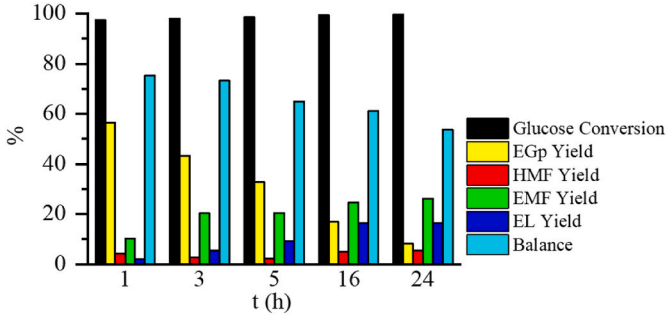

Fig. 6. Conversion and yield values from glucose as a function of reaction time (Experimental conditions: 0.15 g glucose, 0.05 g γ- Al_2O_3, 0.05 g Purolite CT275DR and 140 °C).

3.4.1. *Purolite CT275DR and Alumina role and loading optimization*

To gain further insights about the role of each catalyst during the process, the mass ratio between both catalysts, γ-Al_2O_3 and Purolite CT275DR, was modified (Fig. 7).

For these experiments, one of the catalyst loading was kept constant (0.05 g), while the other was varied between 0.025 and 0.15 g. In addition, for comparison, the result obtained by using the same loading for both catalysts was included. First, the amount of Purolite CT275DR added was modified, keeping the alumina loading constant (Fig. 7a). It can be observed that this change did not affect the results significantly. Glucose conversion was almost complete (98%) in all cases. Likewise, the ethylglucoside yield (45%) was similar, despite varying Purolite CT275DR loading six-fold. In the case of EMF, similar values of yield were attained, although a maximum can be detected when 0.05 g (2:2 wt ratio) of Purolite CT275DR were employed.

Nevertheless, EL yield experienced a notable increase, from 3%, when using 1:2 mass ratio of catalysts, to an 11%, with a 6:2 mass ratio,

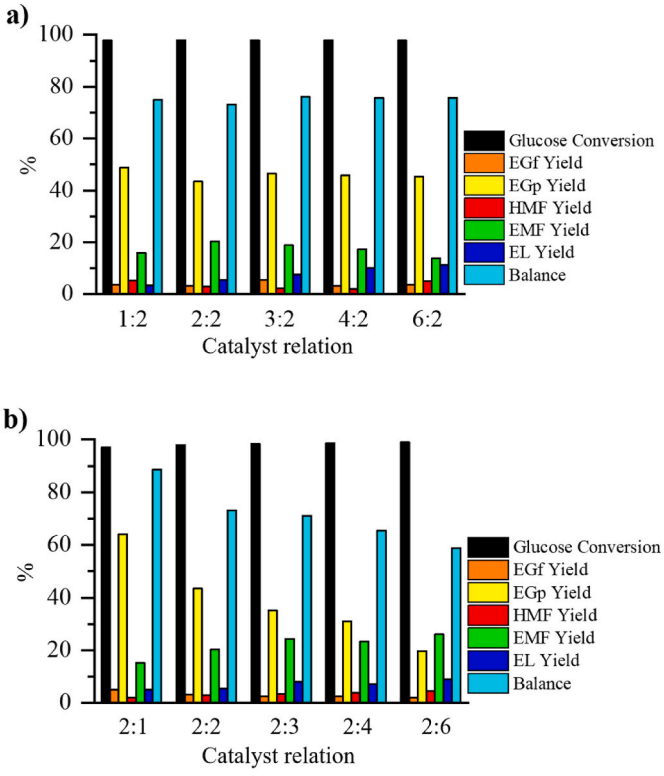

Fig. 7. Glucose conversion and product yields, varying the Purolite CT275DR:γ-Al_2O_3 weight ratio, (a) Keeping constant the loading of Alumina (0.05 g) and (b) keeping constant the loading of Purolite (0.05 g) (Experimental conditions: 0.15 g glucose, 140 °C and 3 h).

after 3 h of reaction. These results could indicate that Brønsted acid sites are present in the reaction in a large excess. Thus, modifying the quantity of Purolite CT275DR added to the reaction medium did not affect substantially the product distribution. Only EMF and, mainly, EL were affected, after modifying the amount of sulfonated polymer, because their strong Brønsted acid sites favoured the rehydration of the furan compounds (HMF and EMF), not detecting any effect on glucose conversion, nor the yield of ethylglucoside, since the Lewis acid sites were the ones limiting them.

However, the trend was different when the loading of alumina was modified (Fig. 7b), since this affected glucose conversion and ethylglucoside yield. Thus, the combined yield of glucose plus EGp is 73% when 0.025 g of alumina were added (Purolite CT275DR:γ-Al_2O_3 2:1 mass ratio) instead of 0.05 g (2:2 wt ratio). Nevertheless, when 0.15 g of alumina (mass ratio of 2:6) were added instead, glucose and all EG only accounted for 21% yield. Most notably, EGp was produced in a 65% yield when the lowest quantity of alumina was employed, and that value decreased progressively as added alumina was raised until there was only a 19% EGp yield when a mass ratio of 2:6 was utilized.

Likewise, HMF, EMF and EL yields showed signs of improvement, increasing from 3, 20 and 5% (2:2 mass ratio) to 5, 26 and 9% (2:6 mass ratio), respectively. However, as was expected, this enhancement was very small, since Lewis acid sites of alumina mainly contributed to isomerization reaction as was previously observed (Fig. S9), which agrees with glucose conversion and EGp yields detected in this case.

3.4.2. *Reutilization of the catalysts*

For reuse tests, given that the system was mostly insensitive to the amount of resin added, but the amount of alumina strongly influenced the product distribution, as was previously observed, 0.05 g of Purolite CT275DR and 0.1 g of alumina were added (Fig. 8), so that any loss of alumina between cycles would not translate in complete loss of the ability to transform the aldose into EMF.

In the case of reusing the combination of catalysts (Fig. 8a), glucose conversion basically unaffected between catalytic runs, decreasing only slightly from 98% after 1st run, to 97% in the fifth. Regarding product distribution, it should be noted that, after four reuses, the ethylglucoside yield rose between experiments, which could be due to a possible deactivation of alumina catalyst. Thus, a steadily increasing lack of Lewis acid sites severely hindered the wanted glucose transformations towards furan derivatives and, consequently, the etherification of glucose gained importance. Moreover, EMF and EL yields fell from 16 to 8% to 9 and 4%, respectively, after 5 catalytic runs. Therefore, Lewis acid sites are essential for the isomerization reaction and subsequent EMF production, in such a way that these vulnerable sites limited the reuse test and reduced the final EMF yield obtained after several catalytic runs.

The fact that the deactivation of alumina, and not the deactivation of Purolite CT275DR, is behind the loss of the capacity of the mixture of catalysts to convert glucose and, subsequently, produce EMF, was demonstrated with reutilization tests of each catalyst separately. When 0.1 g of alumina was only employed in 5 catalytic runs with 0.15 g of glucose, at 140 °C for 3 h (Fig. 8b), the ability of alumina to produce EGp was deteriorated until barely any EGp could be detected. Instead, the EGf yield increased progressively as the catalysts lost the capacity to isomerize the furanose to the pyranose form. On the other hand, HMF yield decreased along catalytic cycles. When the used catalyst after 5 catalytic runs was analysed by thermogravimetry (Fig. S10), it was found to have a 16.0% weight loss between 130 °C and 600 °C due to the carbonaceous deposits formed over the material, compared to barely 1% found in the fresh catalyst. By N_2 adsorption-desorption isotherms, a decrease in the specific surface area from 158 $m^2\ g^{-1}$ in the fresh alumina, to 75 $m^2\ g^{-1}$ was observed. Moreover, a carbon content of 19.8 wt% was found on the surface of alumina by XPS, after these catalytic runs. It has also been reported that both sugars and HMF are susceptible to form humins during dehydration processes [56,60]. EMF, on the other hand, is less prone to humins formation due to the protection of the hydroxyl group as an ether, as pointed out by Zhong et al. [56]. Therefore, Lewis acid sites of alumina were partially blocked by carbonaceous deposits, thus decreasing the HMF production.

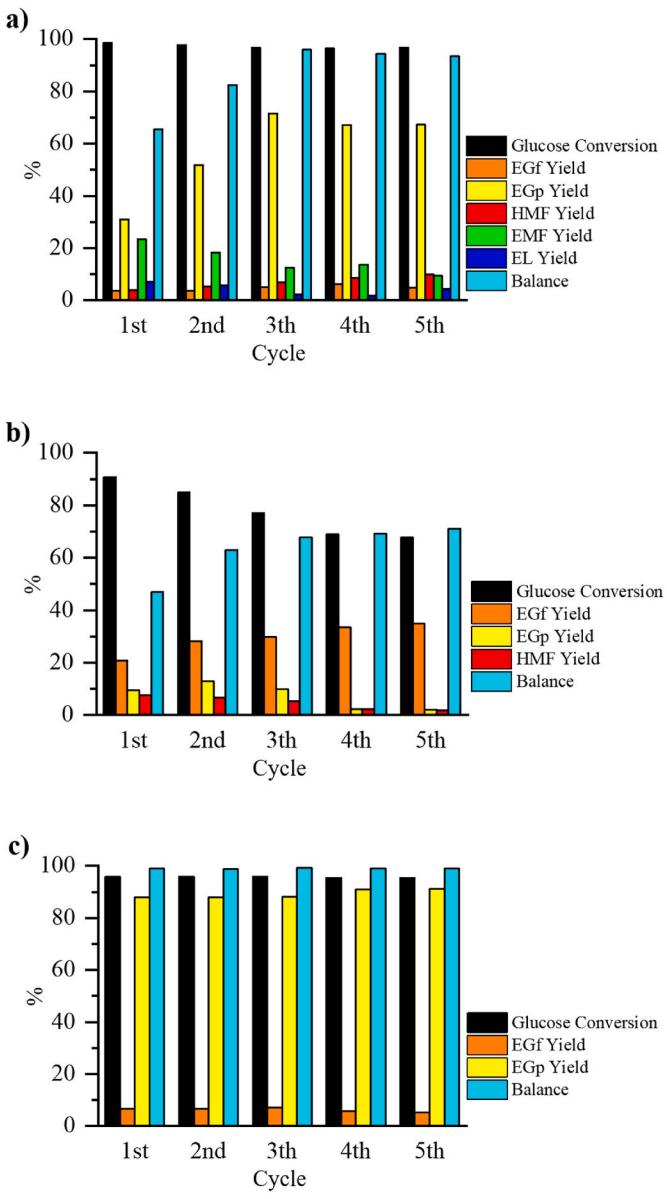

Fig. 8. Glucose conversion and product yields in the reusing study, by using a) 0.05 g of Purolite CT275DR and 0.1 g of γ-Al_2O_3, b) 0.1 g of Alumina, c) 0.05 g of Purolite CT275DR (Experimental conditions: 250 rpm, 140 °C and 3 h).

On the other hand, when only Purolite CT275DR was employed in the reusability runs (Fig. 8c), the material performed in an identical way in each of the five runs performed, with around 89% yield towards EGp and a smaller 6% yield of EGf. This gives us valuable insight in the reaction path followed by glucose in the production of EMF. First, it becomes clear that both, Lewis and Brønsted acid sites are able to catalyse the etherification of D-Glucopyranose, although the weaker acid sites of alumina lead to the formation of great quantities of the furanoside, while the stronger sites in the Purolite transform it quickly in the pyranose form and equilibrium between both forms is achieved. After each cycle in the presence of alumina, in addition of its deactivation, as it has been commented, part of catalyst that remained in suspension was lost, and therefore the number of active sites in the medium decreased. Neither the furanoside nor the pyranoside form can be dehydrated in the

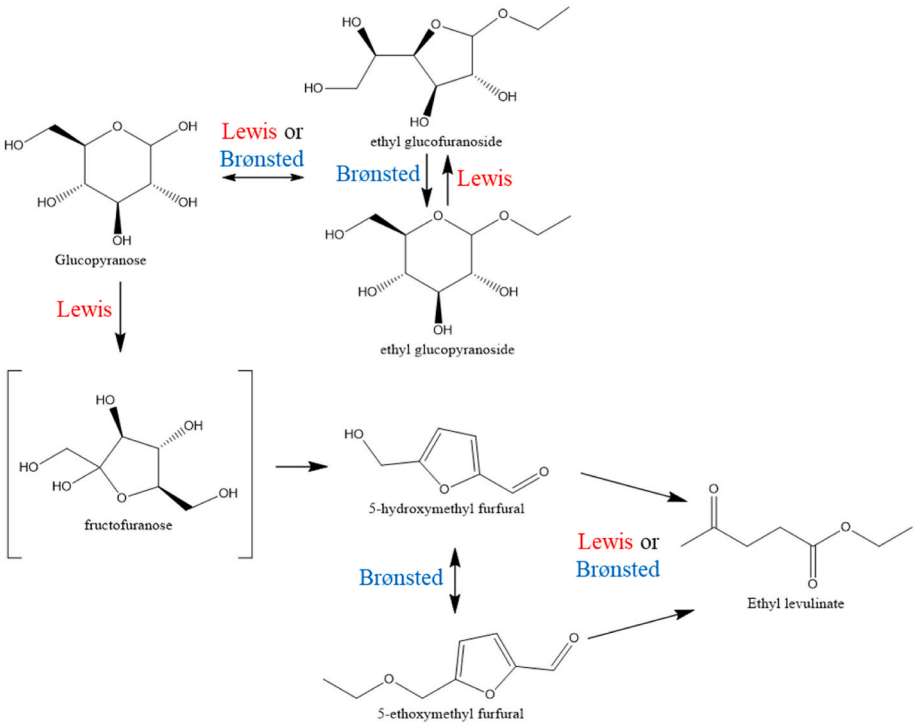

Fig. 9. Simplified reaction pathway followed in etherification from aldoses to ethyl levulinate, together with type of acid site needed for the transformation.

presence of the Brønsted acid sites, or the EMF yield in would not have decreased between cycles in Fig. 9a, as furanosides are present in great quantity, even in the fifth cycle of the alumina catalysts. Therefore, the Lewis acid sites in the alumina must promote the formation of intermediate, probably fructose, as it has been reported in the literature, that is then quickly dehydrated by a the Purolite CT275DR.

3.4.3. Pathways followed by conversion of hexoses in the presence of Purolite CT275DR and alumina catalysts

The following processes have been identified in the transformation of glucose to EMF. Glucose was etherified forming the intermediate EGf, as this is isomer is kinetically favoured to be formed over EGp. The furanoside is, however, less stable than the pyranoside, and isomerization takes place quickly, specially in the presence of strong Brønsted acid sites, to form the ethyl glucopyranoside. As it could be seen in our experiments, both Lewis and Brønsted acid sites can catalyse the formation of both glucosides. However, both compounds are very stable and reaction does not seem to advance. Therefore, the HMF and, subsequently, EMF production would take place from glucose by another pathway. In general, the isomerization of glucose into fructose and subsequent dehydration to HMF has been widely proposed. Guo et al. proposed a mechanism in with glucose could be dehydrated directly to HMF following ring opening. In an alternative pathway, the enediol intermediate could form fructose, that dehydrated to HMF after the loss of 3 water molecules [61]. In the mechanism shown by Zang et al., ethyl glucosides could evolve to EMF via ethyl fructosides, but glucose could also isomerize in the media to fructose, and this fructose could dehydrate with the appropriate acid sites [46]. Therefore, it would be plausible that dehydration of glucose to HMF took place via fructose due to Lewis acid sites coming from alumina promoted this isomerization reaction. Thus, fructose would be quickly transformed to HMF, which could be etherified in the presence of Brønsted acid sites (Fig. 9). HMF etherification to EMF required of very strong Brønsted acid sites, such as those provided by sulfonic groups. It could be observed how alumina was able to carry out the dehydration of fructose to HMF at 140 °C, but still no EMF could be detected, meaning that the HMF is unable to be etherified on the active Lewis acid sites of the alumina catalyst. Chen et al. proposed that glucose could dehydrate to form EMF through the treatment of ethyl glucoside with Brønsted acid sites, in contrast with our observed results. Moreover, they indicate that Lewis acid sites are also suitable for the etherification of HMF to EMF [62].

4. Conclusions

Several sulfonated polymers (Purolite CT275DR, CT269DR, PD206 and Amberlyst-15DRY) have been employed in the etherification of HMF to EMF. Purolite CT275DR and Purolite PD206 exhibited the highest activity and selectivity values for EMF and EL production, due to both their higher surface sulphur content and swelling capacity. Thus, a higher amount of acid sites was exposed to the reactant molecules. Concretely, Purolite CT275DR produced the most promising results using HMF as feedstock: 63% EMF yield after 16 h at 100 °C. Although the fructose could be transformed to EMF with a 50% yield, after 24 h at 100 °C, in the presence of Brønsted acid sites of Purolite CT275DR, this catalyst promoted the etherification of aldose sugars, such as glucose or galactose, to provide the corresponding ethylglucosides and ethylgalactosides, respectively, not being able to isomerize glucose to fructose, and, consequently, HMF can't be formed, neither EMF.

After the addition of alumina, together with the ion-exchange resin, both glucose and galactose could be transformed to EMF and EL (26 and 8% yields, respectively) after 3 h at 140 °C, from galactose, and 26 and 16% yield, respectively, after 24 h at 140 °C, from glucose. Lewis acid sites existing in alumina promoted the glucose isomerization, facilitating the HMF production and its subsequent transformation into EMF. Therefore, both Brønsted and Lewis acid sites are required to produce EMF from aldoses. In the reusability test, it was found that EMF yield decreased between cycles due to carbonaceous deposits and catalyst loss between cycles found for alumina, while the Purolite CT275DR retained its full activity along catalytic runs.

CRediT authorship contribution statement

Benjamín Torres-Olea: Investigation, Formal analysis, Writing – review & editing. **Inmaculada Fúnez-Núñez:** Investigation. **Cristina**

García-Sancho: Conceptualization, Investigation, Writing – review & editing, Supervision, Funding acquisition. **Juan Antonio Cecilia:** Conceptualization, Writing – review & editing. **Ramón Moreno-Tost:** Conceptualization, Writing – review & editing, Supervision. **Pedro Maireles-Torres:** Conceptualization, Resources, Writing – review & editing, Funding acquisition, Project administration, Supervision.

Declaration of competing interest

The authors declare that they have no known competing financial interests or personal relationships that could have appeared to influence the work reported in this paper.

Acknowledgments

This research was funded by the Spanish Ministry of Innovation, Science and Universities (RTI2018-094918-B-C44), FEDER (European Union) funds (RTI2018-094918-B-C44 and UMA18-FEDERJA-171) and Malaga University. Authors thank to Universidad de Málaga/CBUA for funding for open access charge. C.G.S. acknowledges FEDER funds for her postdoctoral contract (UMA18-FEDERJA-171). B.T.O. acknowledges the Ministerio de Universidades for his predoctoral contract (FPU20/02334).

Appendix A. Supplementary data

Supplementary data to this article can be found online at https://doi.org/10.1016/j.renene.2023.03.036.

References

[1] A.D. Moreno, A. Susmozas, J.M. Oliva, M.J. Negro, Overview of bio-based industries, in: Biobased Prod. Ind., 2020, pp. 1–40, https://doi.org/10.1016/b978-0-12-818493-6.00001-4.
[2] P. Basu, Biomass gasification, pyrolysis and torrefaction: practical design and theory, in: Biomass Gasification, Pyrolysis Torrefaction Pract. Des. Theory, second ed., 2013, pp. 1–530, https://doi.org/10.1016/B978-0-12-396488-5.00001-0.
[3] R.-J. van Putten, J.C. van der Waal, E. de Jong, C.B. Rasrendra, H.J. Heeres, J.G. de Vries, Hydroxymethylfurfural, A versatile platform chemical made from renewable resources, Chem. Rev. 113 (2013) 1499–1597, https://doi.org/10.1021/cr300182k.
[4] C.H. Zhou, X. Xia, C.X. Lin, D.S. Tong, J. Beltramini, Catalytic conversion of lignocellulosic biomass to fine chemicals and fuels, Chem. Soc. Rev. 40 (2011) 5588–5617, https://doi.org/10.1039/c1cs15124j.
[5] N. Wei, J. Quarterman, Y.S. Jin, Marine macroalgae: an untapped resource for producing fuels and chemicals, Trends Biotechnol. 31 (2013) 70–77, https://doi.org/10.1016/j.tibtech.2012.10.009.
[6] A.J. Wargacki, E. Leonard, M.N. Win, D.D. Regitsky, C.N.S. Santos, P.B. Kim, S. R. Cooper, R.M. Raisner, A. Herman, A.B. Sivitz, A. Lakshmanaswamy, Y. Kashiyama, An Engineered Microbial Platform for Direct Biofuel Production from Brown Macroalgae, 230502, 2012, pp. 308–314, https://doi.org/10.1126/science.1214547.
[7] M. Mascal, E.B. Nikitin, Towards the efficient, total Glycan utilization of biomass, ChemSusChem 2 (2009) 423–426, https://doi.org/10.1002/cssc.200900071.
[8] J. He, H. Li, Y.M. Lu, Y.X. Liu, Z.B. Wu, D.Y. Hu, S. Yang, Cascade catalytic transfer hydrogenation-cyclization of ethyl levulinate to γ-valerolactone with Al-Zr mixed oxides, Appl. Catal. Gen. 510 (2016) 11–19, https://doi.org/10.1016/j.apcata.2015.10.049.
[9] L. Jiang, L. Zhou, J. Chao, H. Zhao, T. Lu, Y. Su, X. Yang, J. Xu, Direct catalytic conversion of carbohydrates to methyl levulinate: synergy of solid BrØnsted acid and Lewis acid, Appl. Catal. B Environ. 220 (2018) 589–596, https://doi.org/10.1016/j.apcatb.2017.08.072.
[10] T. Xiao, X. Liu, G. Xu, Y. Zhang, Phase tuning of ZrO2 supported cobalt catalysts for hydrodeoxygenation of 5-hydroxymethylfurfural to 2,5-dimethylfuran under mild conditions, Appl. Catal. B Environ. 295 (2021), 120270, https://doi.org/10.1016/j.apcatb.2021.120270.
[11] G.J.M. Gruter, D. Frits, Method for the Synthesis of 5-alkoxymethyl Furfural Ethers and Their Use, 2011. US 2011/0082304 A1.
[12] H. Hafizi, G. Walker, M.N. Collins, Efficient production of 5-ethoxymethylfurfural from 5-hydroxymethylfurfural and carbohydrates over lewis/brønsted hybrid magnetic dendritic fibrous silica core-shell catalyst, Renew. Energy 183 (2021), https://doi.org/10.1016/j.renene.2021.11.036.
[13] C.M. Lew, N. Rajabbeigi, M. Tsapatsis, One-pot synthesis of 5-(Ethoxymethyl) furfural from glucose using Sn-BEA and Amberlyst catalysts, Ind. Eng. Chem. Res. 51 (2012) 5364–5366, https://doi.org/10.1021/ie2025536.
[14] M. Mascal, E.B. Nikitin, Dramatic advancements in the saccharide to 5-(chloromethyl)furfural conversion reaction, ChemSusChem 2 (2009) 859–861, https://doi.org/10.1002/cssc.200900136.
[15] M. Mascal, E.B. Nikitin, Direct, high-yield conversion of cellulose into biofuel, Angew. Chem. Int. Ed. 47 (2008) 7924–7926, https://doi.org/10.1002/anie.200801594.
[16] F. Yang, J. Tang, R. Ou, Z. Guo, S. Gao, Y. Wang, X. Wang, L. Chen, A. Yuan, Fully catalytic upgrading synthesis of 5-Ethoxymethylfurfural from biomass-derived 5-Hydroxymethylfurfural over recyclable layered-niobium-molybdate solid acid, Appl. Catal. B Environ. 256 (2019), 117786, https://doi.org/10.1016/j.apcatb.2019.117786.
[17] H. Hafizi, G. Walker, J. Iqbal, J.J. Leahy, M.N. Collins, Catalytic etherification of 5-hydroxymethylfurfural into 5-ethoxymethyfurfural over sulfated bimetallic SO42−/Al-Zr/KIT-6, a Lewis/Brønsted acid hybrid catalyst, Mol. Catal. 496 (2020), 111176, https://doi.org/10.1016/j.mcat.2020.111176.
[18] J. Dai, Z. Liu, Y. Hu, S. Liu, L. Chen, T. Qi, H. Yang, L. Zhu, C. Hu, Adjusting the acidity of sulfonated organocatalyst for the one-pot production of 5-ethoxymethylfurfural from fructose, Catal. Sci. Technol. 9 (2019) 483–492, https://doi.org/10.1039/c8cy02010h.
[19] B. Liu, Z. Zhang, One-pot conversion of carbohydrates into 5-ethoxymethylfurfural and ethyl d-glucopyranoside in ethanol catalyzed by a silica supported sulfonic acid catalyst, RSC Adv. 3 (2013) 12313–12319, https://doi.org/10.1039/c3ra41043a.
[20] Y. Yang, M.M. Abu-Omar, C. Hu, Heteropolyacid catalyzed conversion of fructose, sucrose, and inulin to 5-ethoxymethylfurfural, a liquid biofuel candidate, Appl. Energy 99 (2012) 80–84, https://doi.org/10.1016/j.apenergy.2012.04.049.
[21] L. Bing, Z. Zhang, K. Deng, Efficient one-pot synthesis of 5-(ethoxymethyl)furfural from fructose catalyzed by a novel solid catalyst, Ind. Eng. Chem. Res. 51 (2012) 15331–15336, https://doi.org/10.1021/ie3020445.
[22] P.K. Kumari, B.S. Rao, D. Mallesh, N. Lingaiah, Niobium exchanged tungstophosphoric acid supported on titania catalysts for selective synthesis of 5-ethoxymethylfurfural from fructose, Mol. Catal. 508 (2021), 111607, https://doi.org/10.1016/j.mcat.2021.111607.
[23] M. Zuo, W. Jia, Y. Feng, X. Zeng, X. Tang, Y. Sun, L. Lin, Effective selectivity conversion of glucose to furan chemicals in the aqueous deep eutectic solvent, Renew. Energy 164 (2021) 23–33, https://doi.org/10.1016/j.renene.2020.09.019.
[24] Y. Román-Leshkov, M. Moliner, J.A. Labinger, M.E. Davis, Mechanism of glucose isomerization using a solid lewis acid catalyst in water, Angew. Chem. Int. Ed. 49 (2010) 8954–8957, https://doi.org/10.1002/anie.201004689.
[25] H. Li, S. Saravanamurugan, S. Yang, A. Riisager, Direct transformation of carbohydrates to the biofuel 5-ethoxymethylfurfural by solid acid catalysts, Green Chem. 18 (2016) 726–734, https://doi.org/10.1039/c5gc01043h.
[26] H. Xin, T. Zhang, W. Li, M. Su, S. Li, Q. Shao, L. Ma, Dehydration of glucose to 5-hydroxymethylfurfural and 5-ethoxymethylfurfural by combining Lewis and Brønsted acid, RSC Adv. 7 (2017) 41546–41551, https://doi.org/10.1039/c7ra07684c.
[27] S. Brunauer, P.H. Emmett, E. Teller, Adsorption of gases in multimolecular layers, J. Am. Chem. Soc. 60 (1938) 309–319, https://doi.org/10.1021/ja01269a023.
[28] J. Landers, G.Y. Gor, A.V. Neimark, Density functional theory methods for characterization of porous materials, Colloids Surfaces A Physicochem. Eng. Asp. 437 (2013) 3–32, https://doi.org/10.1016/j.colsurfa.2013.01.007.
[29] M. Liu, S. Jia, Y. Gong, C. Song, X. Guo, Effective hydrolysis of cellulose into glucose over sulfonated sugar-derived carbon in an ionic liquid, Ind. Eng. Chem. Res. 52 (2013) 8167–8173, https://doi.org/10.1021/ie400571e.
[30] R.M.A. Saboya, J.A. Cecilia, C. García-Sancho, A.V. Sales, F.M.T. de Luna, E. Rodríguez-Castellón, C.L. Cavalcante, Synthesis of biolubricants by the esterification of free fatty acids from castor oil with branched alcohols using cationic exchange resins as catalysts, Ind. Crop. Prod. 104 (2017) 52–61, https://doi.org/10.1016/j.indcrop.2017.04.018.
[31] P. Sundberg, R. Larsson, B. Folkesson, On the core electron binding energy of carbon and the effective charge of the carbon atom, J. Electron. Spectrosc. Relat. Phenom. 46 (1988) 19–29, https://doi.org/10.1016/0368-2048(88)80002-1.
[32] R.M.A. Saboya, J.A. Cecilia, C. García-Sancho, A.V. Sales, F.M.T. de Luna, E. Rodríguez-Castellón, C.L. Cavalcante, Assessment of commercial resins in the biolubricants production from free fatty acids of castor oil, Catal. Today 279 (2017) 274–285, https://doi.org/10.1016/j.cattod.2016.02.020.
[33] R. Soto, C. Fité, E. Ramírez, M. Iborra, J. Tejero, Catalytic activity dependence on morphological properties of acidic ion-exchange resins for the simultaneous ETBE and TAEE liquid-phase synthesis, React. Chem. Eng. 3 (2018) 195–205, https://doi.org/10.1039/c7re00177k.
[34] I. Agirrezabal-Telleria, I. Gandarias, P.L. Arias, Heterogeneous acid-catalysts for the production of furan-derived compounds (furfural and hydroxymethylfurfural) from renewable carbohydrates: a review, Catal. Today 234 (2014) 42–58, https://doi.org/10.1016/j.cattod.2013.11.027.
[35] J. Jae, G.A. Tompsett, A.J. Foster, K.D. Hammond, S.M. Auerbach, R.F. Lobo, G. W. Huber, Investigation into the shape selectivity of zeolite catalysts for biomass conversion, J. Catal. 279 (2011) 257–268, https://doi.org/10.1016/j.jcat.2011.01.019.
[36] A. Penkova, L.F. Bobadilla, F. Romero-Sarria, M.A. Centeno, J.A. Odriozola, Pyridine adsorption on NiSn/MgO-Al 2 O 3 : an FTIR spectroscopic study of surface acidity, Appl. Surf. Sci. 317 (2014) 241–251, https://doi.org/10.1016/j.apsusc.2014.08.093.
[37] J.M.R. Gallo, C. Bisio, G. Gatti, L. Marchese, H.O. Pastore, Physicochemical characterization and surface acid properties of mesoporous [Al]-SBA-15 obtained by direct synthesis, Langmuir 26 (2010) 5791–5800, https://doi.org/10.1021/la903661q.

[38] T. Flannelly, S. Dooley, J.J. Leahy, Reaction pathway analysis of ethyl levulinate and 5-ethoxymethylfurfural from d -fructose acid hydrolysis in ethanol, Energy Fuel. 29 (2015) 7554–7565, https://doi.org/10.1021/acs.energyfuels.5b01481.
[39] P. Che, F. Lu, J. Zhang, Y. Huang, X. Nie, J. Gao, J. Xu, Catalytic selective etherification of hydroxyl groups in 5-hydroxymethylfurfural over H4SiW12O40/MCM-41 nanospheres for liquid fuel production, Bioresour. Technol. 119 (2012) 433–436, https://doi.org/10.1016/j.biortech.2012.06.001.
[40] P. Zhang, J. Yang, H. Hu, D. Hu, J. Gan, Y. Zhang, C. Chen, X. Li, L. Wang, J. Zhang, Catalytic self-etherification of 5-hydroxymethylfurfural to 5,5′(oxy-bis (methylene))bis-2-furfural over zeolite catalysts: effect of pore structure and acidity, Catal. Sci. Technol. 10 (2020) 4684–4692, https://doi.org/10.1039/d0cy00733a.
[41] A.T. Bell, M. Balakrishnan, E.R. Sacia, A.T. Bell, Etherification and reductive etherification of 5-(Hydroxymethyl)furfural: 5-(alkoxymethyl)furfurals and 2,5-bis (alkoxymethyl)furans as potential bio-diesel candidates, Green Chem. 14 (2012) 1626–1634, https://doi.org/10.1039/c2gc35102a.
[42] E.R. Sacia, M. Balakrishnan, A.T. Bell, Biomass conversion to diesel via the etherification of furanyl alcohols catalyzed by Amberlyst-15, J. Catal. 313 (2014) 70–79, https://doi.org/10.1016/j.jcat.2014.02.012.
[43] M.R. Altiokka, H.L. Hoşgün, Kinetics of hydrolysis of benzaldehyde dimethyl acetal over amberlite IR-120, Ind. Eng. Chem. Res. 46 (2007) 1058–1062, https://doi.org/10.1021/ie060716o.
[44] D.C. Sherrington, Preparation, structure and morphology of polymer supports, Chem. Commun. (1998) 2275–2286, https://doi.org/10.1039/a803757d.
[45] M.J. Ginés-Molina, R. Moreno-Tost, J. Santamaría-González, P. Maireles-Torres, Dehydration of sorbitol to isosorbide over sulfonic acid resins under solvent-free conditions, Appl. Catal. Gen. 537 (2017) 66–73, https://doi.org/10.1016/j.apcata.2017.03.006.
[46] L. Zhang, Y. Zhu, L. Tian, Y. He, H. Wang, F. Deng, One-pot alcoholysis of carbohydrates to biofuel 5-ethoxymethylfufural and 5-methoxymethylfufural via a sulfonic porous polymer, Fuel Process. Technol. 193 (2019) 39–47, https://doi.org/10.1016/j.fuproc.2019.05.001.
[47] G. Morales, M. Paniagua, J.A. Melero, J. Iglesias, Efficient production of 5-ethoxymethylfurfural from fructose by sulfonic mesostructured silica using DMSO as co-solvent, Catal. Today 279 (2017) 305–316, https://doi.org/10.1016/j.cattod.2016.02.016.
[48] P. Maneechakr, S. Karnjanakom, Selective conversion of fructose into 5-ethoxymethylfurfural over green catalyst, Res. Chem. Intermed. 45 (2019) 743–756, https://doi.org/10.1007/s11164-018-3640-5.
[49] X. Ge, H. Li, M. Liu, Z. Zhao, X. Jin, X. Fan, X. Gao, Microwave-assisted catalytic alcoholysis of fructose to ethoxymethylfurfural (EMF) over carbon-based microwave-responsive catalyst, Fuel Process. Technol. 233 (2022), 107305, https://doi.org/10.1016/j.fuproc.2022.107305.
[50] T. Dowaki, H. Guo, R.L. Smith, Lignin-derived biochar solid acid catalyst for fructose conversion into 5-ethoxymethylfurfural, Renew. Energy 199 (2022) 1534–1542, https://doi.org/10.1016/j.renene.2022.09.074.
[51] V. Choudhary, S.H. Mushrif, C. Ho, A. Anderko, V. Nikolakis, N.S. Marinkovic, A. I. Frenkel, S.I. Sandler, D.G. Vlachos, Insights into the interplay of lewis and Brønsted acid catalysts in glucose and fructose conversion to 5-(hydroxymethyl) furfural and levulinic acid in aqueous media, J. Am. Chem. Soc. 135 (2013) 3997–4006, https://doi.org/10.1021/ja3122763.
[52] T. Ståhlberg, M.G. Sørensen, A. Riisager, Direct conversion of glucose to 5-(Hydroxymethyl)furfural in ionic liquids with lanthanide catalysts, Green Chem. 12 (2010) 321–332, https://doi.org/10.1039/b916354a.
[53] P. Wrigstedt, J. Keskiväli, M. Leskelä, T. Repo, The role of salts and Brønsted acids in lewis acid-catalyzed aqueous-phase glucose dehydration to 5-hydroxymethylfurfural, ChemCatChem 7 (2015) 501–507, https://doi.org/10.1002/cctc.201402941.
[54] J. Tuteja, S. Nishimura, K. Ebitani, One-pot synthesis of furans from various saccharides using a combination of solid acid and base catalysts, Bull. Chem. Soc. Jpn. 85 (2012) 275–281, https://doi.org/10.1246/bcsj.20110287.
[55] P.F. Pinheiro, D.M. Chaves, M.J. da Silva, One-pot synthesis of alkyl levulinates from biomass derivative carbohydrates in tin(II) exchanged silicotungstates-catalyzed reactions, Cellulose 26 (2019) 7953–7969, https://doi.org/10.1007/s10570-019-02665-w.
[56] R. Zhong, F. Yu, W. Schutyser, Y. Liao, F. de Clippel, L. Peng, B.F. Sels, Acidic mesostructured silica-carbon nanocomposite catalysts for biofuels and chemicals synthesis from sugars in alcoholic solutions, Appl. Catal. B Environ. 206 (2017) 74–88, https://doi.org/10.1016/j.apcatb.2016.12.053.
[57] M.P. Freitas, The anomeric effect on the basis of natural bond orbital analysis, Org. Biomol. Chem. 11 (2013) 2885–2890, https://doi.org/10.1039/c3ob40187a.
[58] P. Lanzafame, D.M. Temi, S. Perathoner, G. Centi, A. MacArio, A. Aloise, G. Giordano, Etherification of 5-hydroxymethyl-2-furfural (HMF) with ethanol to biodiesel components using mesoporous solid acidic catalysts, Catal. Today 175 (2011) 435–441, https://doi.org/10.1016/j.cattod.2011.05.008.
[59] L. Zhang, Y. Liu, R. Sun, S. Yi, Sulfonic acid-functionalized PCP(Cr) catalysts with Cr3+and -SO3H sites for 5-ethoxymethylfurfural production from glucose, RSC Adv. 11 (2021) 33969–33979, https://doi.org/10.1039/d1ra05103b.
[60] T.M.C. Hoang, E.R.H. Van Eck, W.P. Bula, J.G.E. Gardeniers, L. Lefferts, K. Seshan, Humin based by-products from biomass processing as a potential carbonaceous source for synthesis gas production, Green Chem. 17 (2015) 959–972, https://doi.org/10.1039/c4gc01324g.
[61] H. Guo, A. Duereh, Y. Hiraga, X. Qi, R.L. Smith, Mechanism of glucose conversion into 5-ethoxymethylfurfural in ethanol with hydrogen sulfate ionic liquid additives and a lewis acid catalyst, Energy Fuel. 32 (2018) 8411–8419, https://doi.org/10.1021/acs.energyfuels.8b00717.
[62] B. Chen, G. Xu, C. Chang, Z. Zheng, D. Wang, S. Zhang, K. Li, C. Zou, Efficient one-pot production of biofuel 5-ethoxymethylfurfural from corn stover: optimization and kinetics, Energy Fuel. 33 (2019) 4310–4321, https://doi.org/10.1021/acs.energyfuels.9b00357.